

An analysis of PN junctions in piezoelectric semiconductors

Yixun Luo,¹ Chunli Zhang,^{1,2,3,a)} Weiqiu Chen,^{1,2,3} and Jiashi Yang^{1,4,a)}

¹Department of Engineering Mechanics, Zhejiang University, Hangzhou, Zhejiang 310027, China

²Soft Matter Research Center (SMRC), Zhejiang University, Hangzhou 310027, China

³Key Laboratory of Soft Machines and Smart Devices of Zhejiang Province, Hangzhou 310027, China

⁴Department of Mechanical and Materials Engineering, University of Nebraska-Lincoln, Lincoln, Nebraska 68588-0526, USA

(Received 18 July 2017; accepted 21 October 2017; published online 22 November 2017)

We present a theoretical study on the equilibrium state of a PN junction, which is created by two piezoelectric semiconductor half spaces doped oppositely, based on the equations of linear piezoelectricity and the conservation of charge for holes and electrons. The nonlinearity associated with the drift currents of electrons and holes, which appears as products of the unknown carrier concentrations and the unknown electric field, is linearized for small carrier concentration perturbations. An analytical solution is rigorously derived, which is able to show the shaping of the PN junction near the interface. The electromechanical fields and concentrations of electrons and holes near the interface of the PN junction, and the forward-bias current-voltage characteristics of the PN junction under different applied stresses, are calculated and discussed. The effects of a few physical parameters on the properties of the PN junction are investigated as well. *Published by AIP Publishing.* <https://doi.org/10.1063/1.4996754>

I. INTRODUCTION

Piezoelectric semiconductor (PS) materials, which simultaneously possess piezoelectric and semiconducting properties, have attracted considerable attention due to their huge potential applications in future novel multi-functional devices. The wurtzite family semiconductors, such as ZnO, AlN, GaN, and ZnS, are with noncentral symmetry, and hence, they have an electromechanical coupling effect. Recently, various ZnO nanostructures, such as ZnO nanofibers or nanowires, nanotubes, nanobelts, nanospirals, and nanofilms, have been successfully synthesized.^{1–5} They are often made into single structures^{6–9} or arrays^{10–13} and have been used to make nanogenerators for converting mechanical energy into electrical energy,^{14–18} field effect transistors,^{1,2,19} acoustic charge transport devices,²⁰ as well as strain, gas, humidity, and chemical sensors.^{1,21} In the very recent years, there are increasing researches on piezoelectric semiconductor materials and devices. This has changed the landscape of semiconductor devices and formed a new research area called piezotronics.²

The electromechanical and semiconductor properties of piezoelectric semiconductors play a key role in device applications. The basic behaviors of piezoelectric semiconductors can be predicted by a phenomenological theory²² consisting of the equations of linear piezoelectricity²³ and the conservation of charge for electrons and holes.²⁴ However, it normally makes theoretical analyses of piezoelectric semiconductor devices with considerable mathematical challenges owing to piezoelectric semiconductor materials having the properties of anisotropy, electromechanical coupling effect, and the nonlinearity associated with the drift currents of electrons and holes, which are the products of the unknown carrier concentrations

and the unknown electric field.²⁴ In spite of the mathematical difficulties involved, researchers have studied a few useful problems including thickness vibration of plates,^{25,26} propagation of surface waves,²⁷ electromechanical fields in an inclusion,²⁸ fields near cracks,^{29–34} fields and waves in a rod with excessive electrons,^{35,36} static extension of a fiber,^{37,38} and static bending of a fiber.³⁹

A PN junction is the elementary building block of most semiconductor devices, such as diodes, transistors, and LEDs. For traditional PN junctions created by two non-piezoelectric semiconductors, their properties are only dependent on the concentrations of holes, electrons, acceptors, and donors in semiconductors. **PN junctions made of two piezoelectric semiconductors are widely used in many new piezoelectric semiconductor devices.**^{4,5,40} Besides the concentrations of holes, electrons, acceptors, and donors, the polarization potential induced in piezoelectric semiconductors has a significant effect on the properties of PN junctions. **The polarization potential can be utilized to actively tune the performance of PN junction devices.** Therefore, a deep understanding of PN junctions in piezoelectric semiconductor materials and the prediction of the electromechanical fields near a PN junction are fundamentally important to the development of piezoelectric semiconductor devices. To better understand the fundamental mechanism of tuning the performance of PN junction-based piezoelectric semiconductor devices, the researchers presented a simple theoretical model,^{41,42} in which the PN junction consists of piezoelectric and non-piezoelectric semiconducting materials, to predict the piezotronics and piezo-phototronics effect on semiconductor devices. In the developed theory, the semi-coupled model and some assumptions such as the depletion-layer approximation are employed. In this paper, with the fully coupled theory, we theoretically study the basic behaviors of a PN junction between two piezoelectric semiconductors

^{a)}Authors to whom correspondence should be addressed: zhangcl01@zju.edu.cn and jyangl@unl.edu

based on the linear piezoelectric theory and the semiconductor equations. The nonlinearity in the electrons and holes current equations makes it very difficult to obtain an analytical solution. The linearized method is used to analyze the electromechanical fields and the concentrations of electrons and holes in piezoelectric semiconductors. As numerical examples, we investigate the formation of a PN junction between two piezoelectric half spaces and the forward-bias current-voltage characteristics of a PN junction with finite length under different stresses.

II. BASIC EQUATIONS OF PIEZOELECTRIC SEMICONDUCTORS

We use the Cartesian tensor notation. The indices i, j, k, l assume 1, 2, and 3. A comma followed by an index indicates a partial derivative with respect to the coordinate associated with the index. A superimposed dot represents a time derivative. For a piezoelectric semiconductor, the three-dimensional phenomenological theory consists of the equation of motion, the charge equation of electrostatics, and the conservation of charge for holes and electrons (continuity equations)^{43,44}

$$\begin{aligned} T_{ji,j} &= \rho \ddot{u}_i, & D_{i,i} &= q(p - n + N_D^+ - N_A^-), \\ J_{i,i}^p &= -q\dot{p}, & J_{i,i}^n &= q\dot{n}, \end{aligned} \quad (1)$$

where T_{ij} is the stress components, ρ the mass density, u_i the mechanical displacement components, D_i the electric displacement components, $q = 1.6 \times 10^{-19}$ coul the electronic charge, p and n the concentrations of holes and electrons, N_D^+ and N_A^- the concentrations of impurities of donors and accepters, and J_i^p and J_i^n the hole and electron current densities. The carrier recombination processes, such as band-to-band/Auger/R-G center recombination, and the generation processes are also important in semiconductor devices. However, in this paper, we only consider the equilibrium and the steady states, and the net recombination rate is assumed to be zero in the continuity equations of carriers. For piezoelectric semiconductors, the constitutive relations are as follows:^{43,44}

$$\begin{aligned} T_{ij} &= c_{ijkl}S_{kl} - e_{kij}E_k, \\ D_i &= e_{ikl}S_{kl} + \varepsilon_{ik}E_k, \\ J_i^p &= qp\mu_{ij}^pE_j - qD_{ij}^p p_{,j}, \\ J_i^n &= qn\mu_{ij}^nE_j + qD_{ij}^n n_{,j}, \end{aligned} \quad (2)$$

where S_{ij} is the strain components, E_i the electric field components, c_{ijkl} the elastic stiffness, e_{ijk} the piezoelectric constants, ε_{ij} the dielectric constants, μ_{ij}^n and μ_{ij}^p the carrier mobility, and D_{ij}^n and D_{ij}^p the carrier diffusion constants. The strain-displacement relation and the electric field-potential relation are

$$S_{ij} = (u_{i,j} + u_{j,i})/2, \quad E_i = -\varphi_{,i}. \quad (3)$$

The macroscopic behavior of a piezoelectric semiconductor device is inherently governed by Eqs. (1)–(3) with the specific boundary conditions. From these basic equations, the

electromechanical fields in a piezoelectric semiconductor device can be mathematically solved with the boundary conditions and the corresponding continuity conditions at the interface. Mathematically, there are three kinds of boundary conditions, namely, the Dirichlet boundary condition specifying the value of the physical fields, the Neumann boundary condition specifying the value of the normal derivative of the physical fields, and the mixed boundary condition, which includes the foregoing two conditions or their combination. Generally, the boundary conditions and the interfacial continuity conditions are prescribed according to the real physical condition in the modeling of devices. The readers are referred to Refs. 43 and 44 for some typical and representative boundary conditions and the interfacial continuity conditions, which are not summarized here.

As there are nonlinear terms in the last two equations of Eq. (2), which are the electron and hole current equations, it is difficult to obtain an analytical solution. The same linearized method as in Refs. 37 and 38 is employed. Thus, the electron and hole concentrations in the piezoelectric semiconductors are written as

$$n = n_0 + \Delta n, \quad p = p_0 + \Delta p, \quad (4)$$

where

$$n_0 = N_D^+, \quad p_0 = N_A^-, \quad (5)$$

and N_D^+ and N_A^- are constants for uniform impurities, which we assume in this paper. In Eq. (4), Δn and Δp are perturbations of the electron and hole concentrations. Then Eq. (1)₂₋₄ become

$$\begin{aligned} D_{i,i} &= q(\Delta p - \Delta n), \\ q \frac{\partial}{\partial t}(\Delta p) &= -J_{i,i}^p, \\ q \frac{\partial}{\partial t}(\Delta n) &= J_{i,i}^n. \end{aligned} \quad (6)$$

For simplicity, we consider only the case of small Δp and Δn as compared to p_0 and n_0 , which is also called the one-order perturbation method. Consequently, the last two nonlinear equations in Eq. (2)_{3,4} can be linearized as

$$\begin{aligned} J_i^p &= qp_0\mu_{ij}^pE_j - qD_{ij}^p(\Delta p)_{,j}, \\ J_i^n &= qn_0\mu_{ij}^nE_j + qD_{ij}^n(\Delta n)_{,j}. \end{aligned} \quad (7)$$

This type of linearization method was often used in the analysis of piezoelectric semiconductors and ionic conductors before.

III. ONE-DIMENSIONAL PROBLEMS OF PIEZOELECTRIC SEMICONDUCTORS

In this paper, we are mainly interested in ZnO, which belongs to the crystal class of 6mm. Under the compact matrix notation, with r and s ranging from 1 to 6, the material tensors for ZnO can be described by

$$\begin{aligned}
[c_{rs}] &= \begin{pmatrix} c_{11} & c_{12} & c_{13} & 0 & 0 & 0 \\ c_{21} & c_{11} & c_{13} & 0 & 0 & 0 \\ c_{31} & c_{31} & c_{33} & 0 & 0 & 0 \\ 0 & 0 & 0 & c_{44} & 0 & 0 \\ 0 & 0 & 0 & 0 & c_{44} & 0 \\ 0 & 0 & 0 & 0 & 0 & c_{66} \end{pmatrix} \\
[e_{ir}] &= \begin{pmatrix} 0 & 0 & 0 & 0 & e_{15} & 0 \\ 0 & 0 & 0 & e_{15} & 0 & 0 \\ e_{31} & e_{31} & e_{33} & 0 & 0 & 0 \end{pmatrix}, \\
[\varepsilon_{ij}] &= \begin{pmatrix} \varepsilon_{11} & 0 & 0 \\ 0 & \varepsilon_{11} & 0 \\ 0 & 0 & \varepsilon_{33} \end{pmatrix},
\end{aligned} \quad (8)$$

where $c_{66} = (c_{11} - c_{12})/2$. The carrier mobility and diffusion constants of μ_{ij} and D_{ij} have the same structure as ε_{ij} . For convenience, we consider one-dimensional problems of piezoelectric semiconductors here; in this case, all physical fields are assumed to be only dependent on x_3 , and $u_1 = u_2 = 0$. Thus, we have

$$\begin{aligned}
u_3 &= u(x_3, t), \quad \varphi = \varphi(x_3, t), \\
\Delta n &= \Delta n(x_3, t), \quad \Delta p = \Delta p(x_3, t).
\end{aligned} \quad (9)$$

From Eq. (3), the relevant strain and the electric field components are

$$S_{33} = u_{3,3}, \quad E_3 = -\varphi_{,3}. \quad (10)$$

From Eq. (2), the relevant components of T_{ij} , D_i , J_i^p , and J_i^n are

$$T_{33} = c_{33}u_{3,3} + e_{33}\varphi_{,3}, \quad (11)$$

$$D_3 = e_{33}u_{3,3} - \varepsilon_{33}\varphi_{,3}, \quad (12)$$

$$J_3^p = -qp_0\mu_{33}^p\varphi_{,3} - qD_{33}^p(\Delta p)_{,3}, \quad (13)$$

$$J_3^n = -qn_0\mu_{33}^n\varphi_{,3} + qD_{33}^n(\Delta n)_{,3}.$$

With successive substitutions, the relevant ones of Eq. (1) take the following form:

$$\begin{aligned}
c_{33}u_{3,3} + e_{33}\varphi_{,3} &= \rho\ddot{u}_3, \\
e_{33}u_{3,3} - \varepsilon_{33}\varphi_{,3} &= q(\Delta p - \Delta n),
\end{aligned} \quad (14)$$

and

$$\begin{aligned}
\frac{\partial}{\partial t}(\Delta p) &= p_0\mu_{33}^p\varphi_{,3} + D_{33}^p(\Delta p)_{,3}, \\
\frac{\partial}{\partial t}(\Delta n) &= -n_0\mu_{33}^n\varphi_{,3} + D_{33}^n(\Delta n)_{,3}.
\end{aligned} \quad (15)$$

For the equilibrium and the steady states considered in this paper, all the physical fields are independent of time. Thus, Eqs. (14) and (15) reduce to

$$\begin{aligned}
c_{33}u_{3,3} + e_{33}\varphi_{,3} &= 0, \\
e_{33}u_{3,3} - \varepsilon_{33}\varphi_{,3} &= q(\Delta p - \Delta n),
\end{aligned} \quad (16)$$

and

$$\begin{aligned}
p_0\mu_{33}^p\varphi_{,3} + D_{33}^p(\Delta p)_{,3} &= 0, \\
-n_0\mu_{33}^n\varphi_{,3} + D_{33}^n(\Delta n)_{,3} &= 0.
\end{aligned} \quad (17)$$

Equation (16) can be written as

$$u_{3,3} = -\frac{e_{33}}{c_{33}}\varphi_{,3}, \quad -\bar{\varepsilon}_{33}\varphi_{,3} = q(\Delta p - \Delta n), \quad (18)$$

where

$$\bar{\varepsilon}_{33} = \varepsilon_{33} + \frac{e_{33}^2}{c_{33}}. \quad (19)$$

From Eq. (17), we can write

$$(\Delta p)_{,3} = -\frac{p_0\mu_{33}^p}{D_{33}^p}\varphi_{,3}, \quad (\Delta n)_{,3} = \frac{n_0\mu_{33}^n}{D_{33}^n}\varphi_{,3}. \quad (20)$$

Subtracting the two equations in Eq. (20) from each other, we have

$$\varphi_{,3} = -\frac{q}{k^2\bar{\varepsilon}_{33}}(\Delta p - \Delta n)_{,3}, \quad (21)$$

where

$$k^2 = \left(\frac{p_0\mu_{33}^p}{D_{33}^p} + \frac{n_0\mu_{33}^n}{D_{33}^n} \right) \frac{q}{\bar{\varepsilon}_{33}}. \quad (22)$$

k describes, among other things, the competition between conduction and diffusion. Materials with a larger value of k are closer to a conductor. Substituting Eq. (21) into Eq. (18)₂, we obtain a single equation for $\Delta p - \Delta n$

$$(\Delta p - \Delta n)_{,3} = k^2(\Delta p - \Delta n). \quad (23)$$

We can solve Eq. (23) for $\Delta p - \Delta n$

$$\Delta p - \Delta n = C \exp(kx) + B \exp(-kx), \quad (24)$$

then the potential from Eq. (21), and then the displacement and carrier concentrations from Eqs. (18)₁ and (20).

IV. ELECTROMECHANICAL FIELDS ASSOCIATED WITH A PN JUNCTION

We first consider the PN junction between the two piezoelectric half spaces in Fig. 1. We use a prime for the material parameters in the p -doped left half space and a double prime for those in the n -doped region on the right. We treat the two half spaces separately and then apply the boundary conditions at infinity and the jump or continuity conditions at the interface.

For $x_3 < 0$, the physical field is a limit at $-\infty$; we hence have

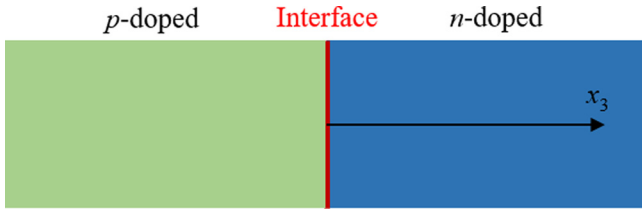


FIG. 1. An interface between two piezoelectric semiconductor half spaces.

$$\Delta p - \Delta n = C_1 \exp(k'x_3). \quad (25)$$

Then, from Eq. (21), the electric potential is given by

$$\varphi = -\frac{q}{(k')^2 \bar{\epsilon}'_{33}} C_1 \exp(k'x_3) + C_2 x_3 + C_3, \quad (26)$$

and, from Eq. (18)₁, the displacement field is

$$u_3 = -\frac{\epsilon'_{33}}{c'_{33}} \left[-\frac{q}{(k')^2 \bar{\epsilon}'_{33}} C_1 \exp(k'x_3) + C_2 x_3 + C_3 \right] + C_4 x_3 + C_5. \quad (27)$$

Since $\Delta p - \Delta n$ is already given by Eq. (25), we only need one from the two equations in Eq. (20). From Eq. (20)₂, we have

$$\Delta n = \frac{n'_0 \mu''_{33}}{D''_{33}} \left[-\frac{q}{(k')^2 \bar{\epsilon}'_{33}} C_1 \exp(k'x_3) + C_2 x_3 + C_3 \right] + C_6 x_3 + C_7. \quad (28)$$

Similarly, for $x_3 > 0$, we have

$$\Delta p - \Delta n = C_8 \exp(-k''x_3), \quad (29)$$

$$\varphi = -\frac{q}{(k'')^2 \bar{\epsilon}''_{33}} C_8 \exp(-k''x_3) + C_9 x_3 + C_{10}, \quad (30)$$

$$u_3 = -\frac{\epsilon''_{33}}{c''_{33}} \left[-\frac{q}{(k'')^2 \bar{\epsilon}''_{33}} C_8 \exp(-k''x_3) + C_9 x_3 + C_{10} \right] + C_{11} x_3 + C_{12}, \quad (31)$$

and

$$\Delta n = \frac{n''_0 \mu''_{33}}{D''_{33}} \left[-\frac{q}{(k'')^2 \bar{\epsilon}''_{33}} C_8 \exp(-k''x_3) + C_9 x_3 + C_{10} \right] + C_{13} x_3 + C_{14}. \quad (32)$$

The fourteen unknown constants C_1, C_2, \dots, C_{14} can be determined from the boundary conditions at infinity and the continuity conditions at the interface. At infinity, the stress, electric current, and electric displacement are zero, and we have the following boundary conditions:

$$\begin{aligned} T_{33}(\pm\infty) &= 0, & D_3(\pm\infty) &= 0, \\ J_3^p(\pm\infty) &= 0, & J_3^n(\pm\infty) &= 0. \end{aligned} \quad (33)$$

For the considered problem, there are two redundant conditions in Eq. (33). They are $T_{33}(\pm\infty) = 0$ (or $D_3(\pm\infty) = 0$). At the interface between the *p*- and *n*-doped regions, the

displacement, stress, potential, electric displacement, current, and concentrations of hole and electron should be continuous, thus we have the following:

$$\begin{aligned} u_3(0^-) &= u_3(0^+), & T_{33}(0^-) &= T_{33}(0^+), \\ \varphi(0^-) &= \varphi(0^+), & D_3(0^-) &= D_3(0^+), \end{aligned} \quad (34)$$

and

$$\begin{aligned} n(0^-) &= n(0^+), & p(0^-) &= p(0^+), \\ J_3^n(0^-) &= J_3^n(0^+), & J_3^p(0^-) &= J_3^p(0^+). \end{aligned} \quad (35)$$

The continuity conditions of $T_{33}(0^-) = T_{33}(0^+)$, $J_3^n(0^-) = J_3^n(0^+)$, and $J_3^p(0^-) = J_3^p(0^+)$ in Eqs. (34) and (35) are automatically satisfied, which are redundant conditions as well. The preceding equations and the boundary/continuity conditions are invariant under a rigid-body displacement in the x_3 direction and a shift of the electric potential through a constant. To fix the rigid-body displacement and the arbitrary constant in the electric potential so that the displacement and potential fields are unique, we choose the interface as a reference for the displacement and the potential and impose

$$u_3(0) = 0, \quad \varphi(0) = 0. \quad (36)$$

To satisfy Eq. (33), we must have

$$C_2 = C_4 = C_6 = C_9 = C_{11} = C_{13} = 0. \quad (37)$$

Then, Eqs. (34)₂ and (35)_{3,4} are also satisfied. We note that in this case the strain and the electric field also vanish at infinity. From Eqs. (26) and (30), we see that $\varphi(\infty) - \varphi(-\infty) = C_{10} - C_3$, which determines the “built-in” junction voltage. There are still eight unknown constants of $C_1, C_3, C_5, C_7, C_8, C_{10}, C_{12}$, and C_{14} . There are seven available conditions in total in Eqs. (34), (35), and (36) left, except for the abovementioned five redundant conditions. The total electrons and holes at the equilibrium state after the formation of PN junction have to be the same as their initial values, which is the condition of the global conservation of holes and electrons. We thus have

$$\int_{-\infty}^{\infty} \Delta n dx_3 = 0, \quad \int_{-\infty}^{\infty} \Delta p dx_3 = 0. \quad (38)$$

With the use of Eqs. (25), (28), (29), and (32), it can be shown that Eq. (38) reduces to the following single equation, which serves as the eighth condition for determining the remaining eight undetermined constants:

$$\frac{n'_0 \mu''_{33}}{D''_{33}} C_3 + C_7 + \frac{n''_0 \mu''_{33}}{D''_{33}} C_{10} + C_{14} = 0. \quad (39)$$

The eight linear algebraic equations are solved on a computer using MATLAB. The electromechanical field in a piezoelectric semiconductor PN junction is analytically derived, which gives a deeper insight into the properties and the formation of the PN junction.

The PN junction-based semiconductor devices are commonly applied a bias voltage. At the steady state, the current flowing through the PN junction as a function of the bias

voltage, which is called the current-voltage characteristic, plays a key role in the device's behavior. The current-voltage characteristics of piezoelectric semiconductor devices have been successfully enhanced and tuned by applying an external mechanical stress or strain.⁴⁵ It is very significant to investigate the effect of the applied stress on the current-voltage characteristics of a PN junction consisting of two piezoelectric semiconductor regions. For a PN junction with length $2L$ under forward bias voltage $2V$, the basic solutions of $C_{15} \exp(-k'x_3)$ and $C_{16} \exp(k''x_3)$ should be added to the general solutions in Eqs. (25) and (29), respectively. As a result, there are sixteen unknown constants. In this case, the boundary conditions are the stresses at the two ends are $T(\pm L) = T_0$, and the electric potential at the two ends are $\varphi(-L) = V$ and $\varphi(L) = -V$. Physically, the incremental carriers and the electric fields at the two ends, which are far away from the PN junction region, can be assumed to be zero.⁴³ We thus have $\Delta n'(-L) = \Delta p''(L) = 0$ and $E'(-L) = E''(L) = 0$. The displacement, potential, electrons, holes, and currents should be continuous at the interface. Hence, the interfacial continuity conditions are $u_3(0^-) = u_3(0^+)$, $\varphi(0^-) = \varphi(0^+)$, $n(0^-) = n(0^+)$, $p(0^-) = p(0^+)$, $J_3^n(0^-) = J_3^n(0^+)$, and $J_3^p(0^-) = J_3^p(0^+)$. In addition, we set $u_3(0) = 0$ to fix the rigid-body displacement so that the displacement is unique. Hence, the sixteen unknown constants can be determined from the above-mentioned sixteen conditions. As a result, the analytical expression of the total current can be directly obtained with a quite similar procedure. The detailed derivation process is not provided here.

V. NUMERICAL RESULTS AND DISCUSSION

In the numerical calculation, we consider the PN junction formed by joining the p-type ZnO and n-type ZnS piezoelectric semiconductor materials. The relevant material constants of ZnO and ZnS are taken from the Appendix in Ref. 23. For ZnO, they are the elastic constant $c_{33} = 210.9$ GPa, piezoelectric constant $e_{33} = 1.32$ C/m², and dielectric constant $\epsilon_{33} = 1.119 \times 10^{-11}$ F/m. For ZnS, the elastic constant $c_{33} = 127.6$ GPa, piezoelectric constant $e_{33} = 0.272$ C/m², and dielectric constant $\epsilon_{33} = 7.703 \times 10^{-11}$ F/m. At room temperature, we have⁴³

$$\frac{\mu_{33}^n}{D_{33}^n} = \frac{\mu_{33}^p}{D_{33}^p} = \frac{q}{k_B T} = 38.46 \text{ V}^{-1}, \quad (40)$$

where k_B is the Boltzmann constant and T the absolute temperature. Equation (40) is the well-known Einstein relation. We consider the following initial carrier concentrations described by step functions (as shown in Fig. 2) before diffusion begins the formation of a PN junction.

The main concern is to understand the formation of the PN junction and the distributions of the electromechanical fields in the PN junction in this paper. The initial carrier concentrations have no effect on the essential behaviors of the electromechanical fields in piezoelectric semiconductors, but only the different initial concentrations change the amplitude of the physical fields. As a numerical example, therefore, we can freely choose the value of the initial concentrations. For

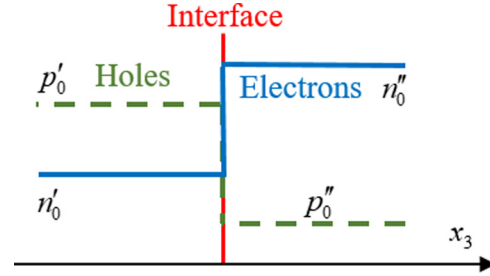


FIG. 2. Sketch of initial carrier concentrations in a PN junction.

convenience, we consider the initial concentrations with some symmetry or anti-symmetry. In this special case, we have $p'_0 = n''_0$ and $p''_0 = n'_0$, and there is the relation of $k''^2/k'^2 = \bar{\epsilon}'_{33}/\bar{\epsilon}''_{33}$. We denote $\alpha = \sqrt{\bar{\epsilon}'_{33}/\bar{\epsilon}''_{33}}$, which is only dependent of the material properties in two regions, and $k'' = \alpha k'$. The undetermined constants are thus found to be

$$\begin{aligned} C_1 &= \frac{2(n'_0 - p'_0)}{1 + \alpha}, & C_3 &= \frac{2(n'_0 - p'_0)}{(1 + \alpha)(n'_0 + p'_0)} \frac{k_B T}{q}, \\ C_5 &= 0, & C_{12} &= 0, \\ C_7 &= \frac{(p'_0 - n'_0)(p'_0 + 3n'_0 + \alpha(n'_0 - p'_0))}{2(1 + \alpha)(n'_0 + p'_0)}, \\ C_8 &= \frac{2\alpha(p'_0 - n'_0)}{1 + \alpha}, & C_{10} &= \frac{2\alpha(p'_0 - n'_0)}{(1 + \alpha)(n'_0 + p'_0)} \frac{k_B T}{q}, \\ C_{14} &= \frac{(n'_0 - p'_0)(p'_0 - n'_0 + \alpha(n'_0 + 3p'_0))}{2(1 + \alpha)(n'_0 + p'_0)}. \end{aligned} \quad (41)$$

In the following calculations, we chose the initial concentrations with $p'_0 = n''_0 = 10 \times 10^{20} \text{ m}^{-3}$ and $p''_0 = n'_0 = 7 \times 10^{20} \text{ m}^{-3}$. The jumps of the step functions are not large, so the assumptions of the linear theory are not violated. It can be seen from Eq. (41) that all these constants vanish when $n'_0 = p'_0$.

Figure 3 shows the plots of various electromechanical fields near the interface. Figures 3(a) and 3(b) give the distributions of the concentrations of holes and electrons at the equilibrium state of the PN junction. It can be seen that the holes and electrons are now continuous at the interface because of diffusion. They are smooth functions after diffusion although they still change rapidly near the interface. The perturbations Δp and Δn of the hole and electron concentrations are shown in Figs. 3(c) and 3(d), respectively, which are discontinuous at the interface of the PN junction. This is because the initial carrier concentrations are discontinuous at the interface, but p and n are continuous. From Figs. 3(c) and 3(d), we can see that the holes from the p-type region near the interface tend to diffuse into the n-type region, and the electrons from the n-type region near the interface tend to diffuse into the p-type region. As a result of the diffusion of the holes and electrons, the positive ions in the n-type region and the negative charged ions in the p-type region are finally formed, respectively, near the interface. The net or total charge increment is plotted in Fig. 3(e). It can be seen that the total charge increment has a sign change there, which physically shows the formation of a PN junction. Figure 3(f) shows the electric field produced by the

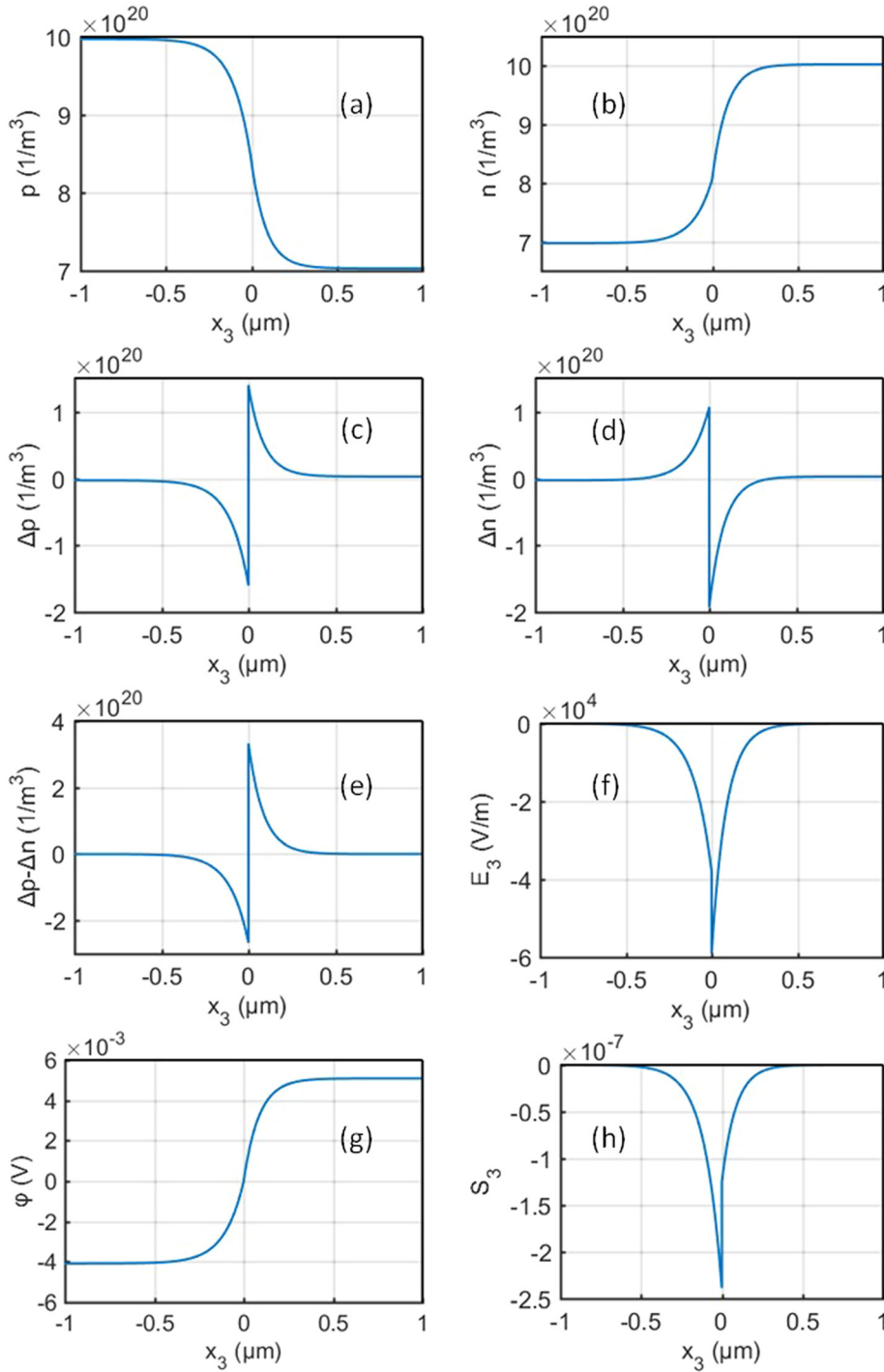


FIG. 3. Fields near the interface. (a) $p(x_3)$ for holes. (b) $n(x_3)$ for electrons. (c) Δp . (d) Δn . (e) $\Delta p - \Delta n$ for the total charge (PN junction). (f) $E_3(x_3)$ for the electric field. (g) $\phi(x_3)$ for the electric potential. (h) $S_3(x_3)$ for the strain.

charges in the PN junction, which is negative (pointing to the left) as expected. Figure 3(g) is the electric potential corresponding to the electric field in Fig. 3(f). The potential in Fig. 3(g) rises from left to right. Since the interface is chosen as a reference where the electric potential is zero, the potential is negative on the left and positive on the right. It changes rapidly near the interface and is essentially constant far away from there. As there is an electromechanical coupling effect in the piezoelectric semiconductor material, there must be a mechanical deformation resulting from the electric field as shown in Fig. 3(f). We plot the strain field in Fig. 3(h) which is localized near the interface.

It can be seen from Eqs. (25) and (29) that $k' = k''/\alpha = k$ is an important combination of parameters. The distributions of the electromechanical fields in the PN junction are dependent on the value of k . For the case of $p'_0 = n'_0 = 10 \times 10^{20} \text{ m}^{-3}$ and $p''_0 = n''_0 = 7 \times 10^{20} \text{ m}^{-3}$ used in the preceding calculations, let

$$k_0^2 = \left(\frac{p_0 \mu_{33}^p}{D_{33}^p} + \frac{n_0 \mu_{33}^n}{D_{33}^n} \right) \frac{q}{\bar{\epsilon}_{33}'} = (p_0 + n_0) \frac{q}{k_B T} \frac{q}{\bar{\epsilon}_{33}'}. \quad (42)$$

Taking the value of k_0 in Eq. (42) as the unit of k , we calculate the electromechanical fields for different values of k , and plot them in Fig. 4. When k varies, $p_0 + n_0$ varies

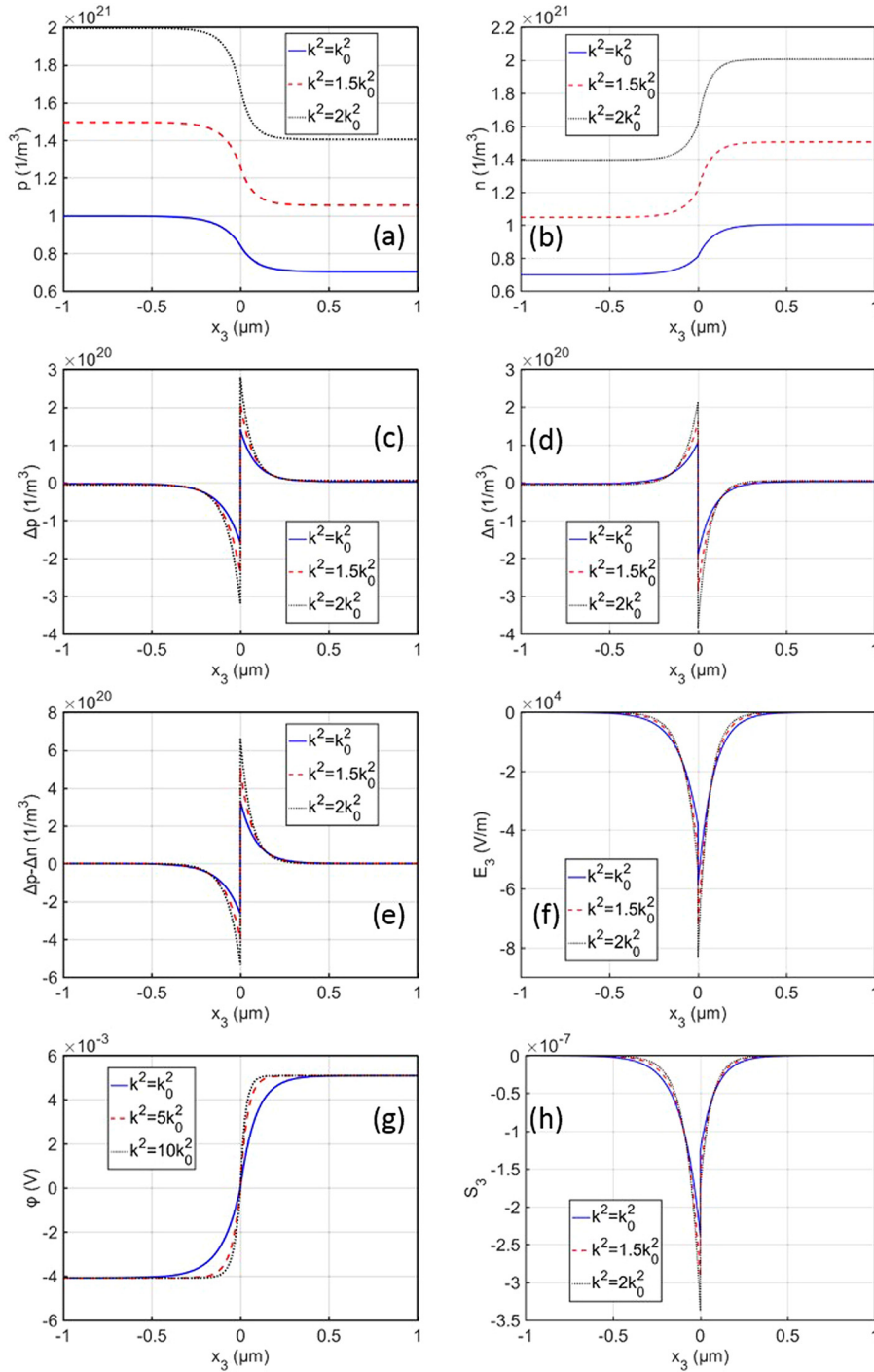


FIG. 4. Effects of k . (a) $p(x_3)$ for holes. (b) $n(x_3)$ for electrons. (c) Δp . (d) Δn . (e) $\Delta p - \Delta n$ for the total charge (PN junction). (f) $E_3(x_3)$ for the electric field. (g) $\phi(x_3)$ for the electric potential. (h) $S_3(x_3)$ for the strain.

effectively when the other parameters are fixed. From Eqs. (25) and (29), we expect that when k increases, the fields vary more rapidly in and near the PN junction. This is shown clearly in the figure. In Figs. 4(a) and 4(b), the curves with larger values of k are higher because of more carriers. Figures 4(c) and 4(d) are the distributions of the incremental holes and electrons, respectively, with different values of k . For the same reason, when k increases, there are more carriers in the PN junction in Fig. 4(e) and larger electric fields in Fig. 4(f). The effects of k on the potential and the strain are shown in Figs. 4(g) and 4(h), respectively.

To study the effects of the initial concentrations of the holes and electrons on the behavior of the PN junction, we

keep $k = k_0$ of Eq. (42) constant and vary the value of the initial carrier concentration difference of $p'_0 - n'_0$. When the initial carrier concentration difference of $p'_0 - n'_0$ increases, the carrier concentrations in Figs. 5(a) and 5(b) change more rapidly as expected. Accordingly, there are more carriers in the PN junction and a larger electric field. The distributions of Δp , Δn , $\Delta p - \Delta n$, E , ϕ , and S_3 with different values of k are plotted in Figs. 5(c)–5(h), respectively. The initial concentrations of the holes and electrons have a significant effect on the distributions of the electromechanical fields and the charge carriers in the PN junction.

Next, we numerically investigate the current-voltage characteristics of a PN junction made of p-type ZnO at the

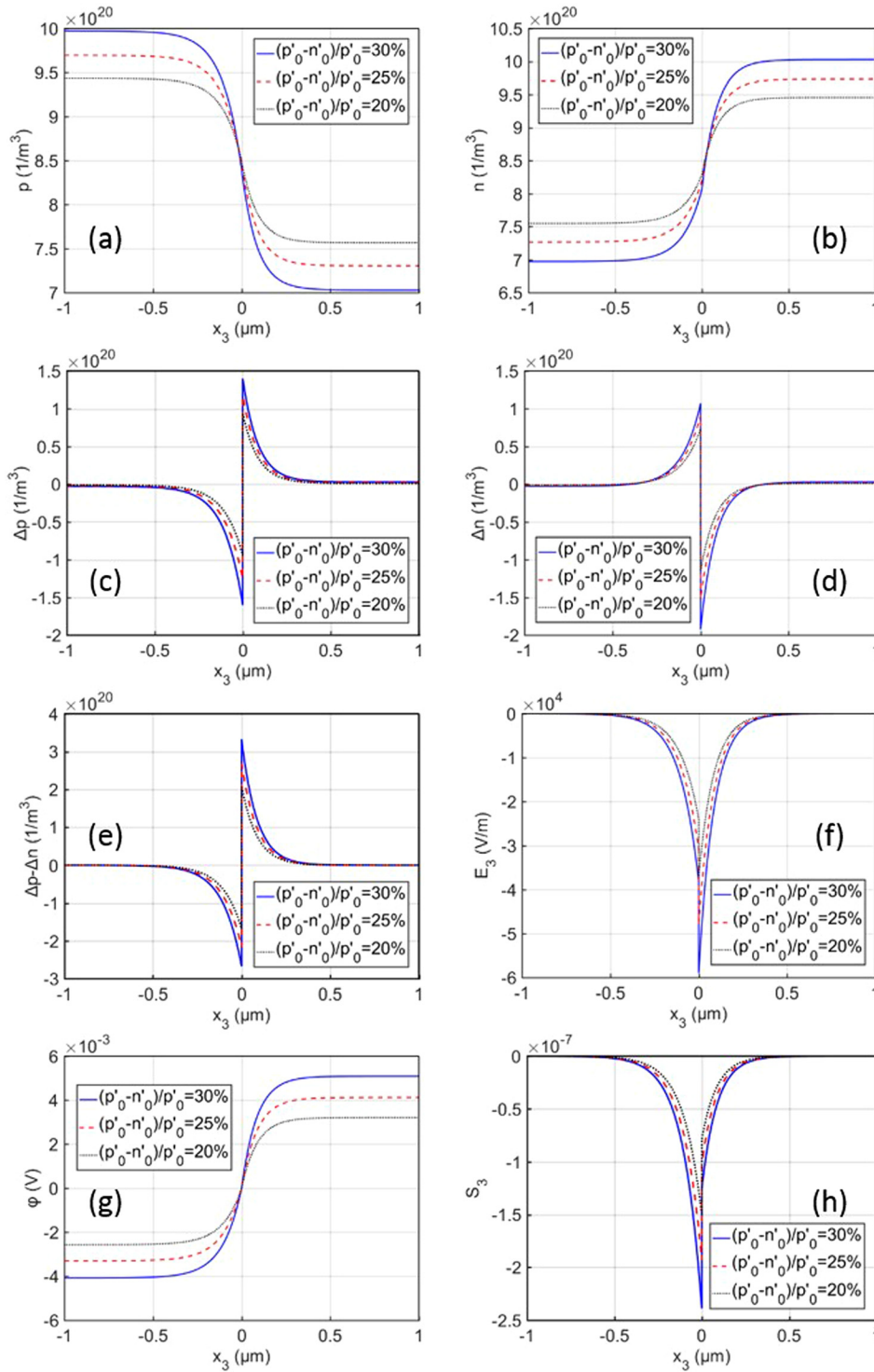


FIG. 5. Effects of initial carrier concentration difference. (a) $p(x_3)$ for holes. (b) $n(x_3)$ for electrons. (c) Δp . (d) Δn . (e) $\Delta p - \Delta n$ for the total charge (PN-junction). (f) $E_3(x_3)$ for the electric field. (g) $\phi(x_3)$ for the electric potential. (h) $S_3(x_3)$ for the strain.

left side and n-type ZnS at the right side under different applied stresses. The two piezoelectric semiconductors have equal length of 50 nm and radius of 10 nm. The carrier concentrations are $n'_0 = 8.5 \times 10^{22} \text{ m}^{-3}$ and $p'_0 = 10^{23} \text{ m}^{-3}$ in the p-type side, and $n''_0 = 10^{23} \text{ m}^{-3}$ and $p''_0 = 8.5 \times 10^{22} \text{ m}^{-3}$ in the n-type side. The forward-bias current-voltage characteristics of the PN junction under different stresses are plotted in Fig. 6(a). It can be seen that the compress stresses enhance the electric current in the PN junction, while the tension stress decreases the electric current. This is because the induced polarization potential or the electric field, resulting from the

piezoelectric effect, changes the effective electric field in the PN junction. The curves in Fig. 6(b) show the effect of the applied stresses on the electric potential distributions under the forward-bias voltage of 2 mV. It should be noted that the proposed theoretical model in this paper can only predict the behavior of the PN junction under small fields. Under small forward-bias voltage, the current-voltage curves are linear as shown in Fig. 6(a), which is a linear approximation of the nonlinear current-voltage relation developed in Ref. 41. It is difficult to obtain the analytical solution of the nonlinear current-voltage relation of the PN junction from the

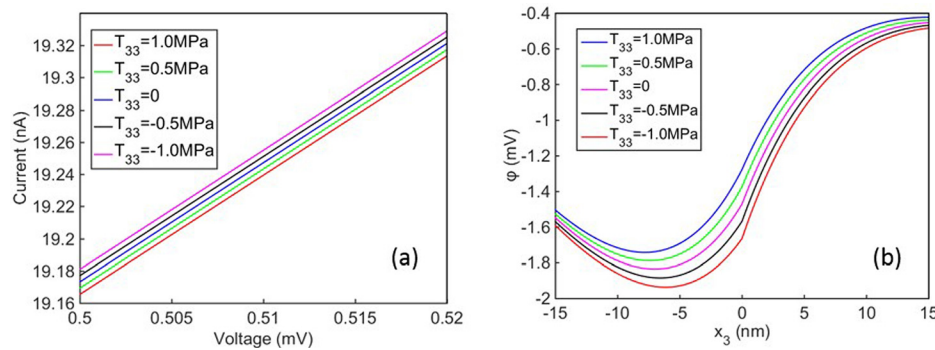


FIG. 6. (a) The current-voltage relations and (b) the electric potential distributions under different applied stresses.

continuum theory. It can be numerically solved with the finite element method and the finite difference method.

VI. CONCLUSION

In this paper, we theoretically investigated the behavior of the PN junction and the forward bias current-voltage characteristics based on the linear equations of piezoelectricity and the conservation of charge. At an interface between two oppositely doped piezoelectric semiconductors, initially discontinuous carrier concentrations described by step functions are found to become continuous and smooth because of diffusion. The carrier concentrations vary rapidly near the interface. The net charge distribution concentrates at the interface and changes sign there and thus forms a PN junction and produces a local electric field. Since the material is piezoelectric, there also exist mechanical fields associated with the PN junction. The linearized phenomenological theory for piezoelectric semiconductors is able to describe the formation of PN junctions and their electromechanical fields when the carrier concentration perturbations are small, which can be useful in the analysis and design of the novel piezoelectric semiconductor or piezotronic devices.

ACKNOWLEDGMENTS

This work was supported by the National Natural Science Foundation of China (Grant Nos. 11672265, 11202182, and 11621062) and the Fundamental Research Funds for the Central Universities (Grant Nos. 2016QNA4026 and 2016XZZX001-05).

- ¹Z. L. Wang, *Adv. Mater.* **15**, 432 (2003).
- ²Z. L. Wang, *Nano Today* **5**, 540 (2010).
- ³B. Kumar and S. W. Kim, *J. Mater. Chem.* **21**, 18946 (2011).
- ⁴K. Y. Lee, B. Kumar, J. S. Seo, K. H. Kim, J. I. Sohn, S. N. Cha, D. Choi, Z. L. Wang, and S. W. Kim, *Nano Lett.* **12**, 1959 (2012).
- ⁵K. Y. Lee, J. Bae, S. M. Kim, J. H. Lee, G. C. Yoon, M. K. Gupta, S. J. Kim, H. Kim, J. J. Park, and S. W. Kim, *Nano Energy* **8**, 165 (2014).
- ⁶Y. F. Gao and Z. L. Wang, *Nano Lett.* **9**, 1103 (2009).
- ⁷Y. F. Hu, Y. L. Chang, P. Fei, R. L. Snyder, and Z. L. Wang, *ACS Nano* **4**, 1234 (2010).
- ⁸R. Araneo, G. Lovat, P. Burghignoli, and C. Falconi, *Adv. Mater.* **24**, 4719 (2012).
- ⁹J. L. Ji, Z. Y. Zhou, X. Yang, W. D. Zhang, S. B. Sang, and P. W. Li, *Small* **9**, 3014 (2013).
- ¹⁰Y. Shen, J. Hong, S. Xu, S. S. Lin, H. Fang, S. Zhang, Y. Ding, R. L. Snyder, and Z. L. Wang, *Adv. Funct. Mater.* **20**, 703 (2010).
- ¹¹T. T. Chen, C. L. Cheng, S. P. Fu, and Y. F. Chen, *Nanotechnology* **18**, 225705 (2007).
- ¹²J. Yoo, C. H. Lee, Y. J. Doh, H. S. Jung, and G. C. Yi, *Appl. Phys. Lett.* **94**, 223117 (2009).
- ¹³H. Z. Xue, N. Pan, M. Li, Y. K. Wu, X. P. Wang, and J. G. Hou, *Nanotechnology* **21**, 215701 (2010).
- ¹⁴P. X. Gao, J. H. Song, J. Liu, and Z. L. Wang, *Adv. Mater.* **19**, 67 (2007).
- ¹⁵M. Y. Choi, D. Choi, M. J. Jin, I. Kim, S. H. Kim, J. Y. Choi, S. Y. Lee, J. M. Kim, and S. W. Kim, *Adv. Mater.* **21**, 2185 (2009).
- ¹⁶G. Romano, G. Mantini, A. D. Garlo, A. D'Amico, C. Falconi, and Z. L. Wang, *Nanotechnology* **22**, 465401 (2011).
- ¹⁷A. Asthana, H. A. Ardakani, Y. K. Yap, and R. S. Yassar, *J. Mater. Chem. C* **2**, 3995 (2014).
- ¹⁸Q. L. Liao, Z. Zhang, X. H. Zhang, M. Mohr, Y. Zhang, and H. J. Fecht, *Nano Res.* **7**, 917 (2014).
- ¹⁹X. D. Wang, J. Zhou, J. H. Song, J. Liu, N. S. Xu, and Z. L. Wang, *Nano Lett.* **6**, 2768 (2006).
- ²⁰S. Buyukkose, A. Hernandez-Minguez, B. Vratzov, C. Somaschini, L. Geelhaar, H. Riechert, W. G. van der Wiel, and P. V. Santos, *Nanotechnology* **25**, 135204 (2014).
- ²¹J. Yu, S. J. Ippolito, W. Wlodarski, M. Strano, and K. Kalantar-Zadeh, *Nanotechnology* **21**, 265502 (2010).
- ²²A. R. Hutson and D. L. White, *J. Appl. Phys.* **33**, 40 (1962).
- ²³B. A. Auld, *Acoustic Fields and Waves in Solids* (John Wiley and Sons, New York, 1973), Vol. I.
- ²⁴R. F. Pierret, *Semiconductor Fundamentals*, 2nd ed. (Addison-Wesley, Massachusetts, 1988).
- ²⁵J. Wauer and S. Suherman, *Int. J. Eng. Sci.* **35**, 1387 (1997).
- ²⁶P. Li, F. Jin, and J. S. Yang, *Smart Mater. Struct.* **24**, 025021 (2015).
- ²⁷C. L. Gu and F. Jin, *Philos. Mag. Lett.* **95**, 92 (2015).
- ²⁸J. S. Yang, Y. C. Song, and A. K. Soh, *Arch. Appl. Mech.* **76**, 381 (2006).
- ²⁹Y. T. Hu, Y. Zeng, and J. S. Yang, *Int. J. Solids Struct.* **44**, 3928 (2007).
- ³⁰J. Sladek, V. Sladek, E. Pan, and D. L. Young, *Comput. Model. Eng. Sci.* **99**, 273 (2014).
- ³¹J. Sladek, V. Sladek, E. Pan, and M. Wünsche, *Eng. Fract. Mech.* **126**, 27 (2014).
- ³²M. H. Zhao, Y. B. Pan, C. Y. Fan, and G. T. Xu, *Int. J. Solids Struct.* **94-95**, 50 (2016).
- ³³C. Y. Fan, Y. Yan, G. T. Xu, and M. H. Zhao, *Eng. Fract. Mech.* **165**, 183 (2016).
- ³⁴M. H. Zhao, Y. Li, Y. Yan, and C. Y. Fan, *Eng. Anal. Boundary Elem.* **67**, 115 (2016).
- ³⁵C. L. Zhang, X. Y. Wang, W. Q. Chen, and J. S. Yang, *J. Zhejiang Univ., Sci., A* **17**, 37 (2016).
- ³⁶C. L. Zhang, X. Y. Wang, W. Q. Chen, and J. S. Yang, *AIP Adv.* **6**(4), 045301 (2016).
- ³⁷C. L. Zhang, X. Y. Wang, W. Q. Chen, and J. S. Yang, *Smart Mater. Struct.* **26**, 025030 (2017).
- ³⁸C. L. Zhang, Y. X. Luo, R. R. Cheng, and X. Y. Wang, *MRS Adv.* **2**, 3421-3426 (2017).
- ³⁹Y. F. Gao and Z. L. Wang, *Nano Lett.* **7**, 2499 (2007).
- ⁴⁰S. Y. Chung, S. Kim, J. H. Lee, K. Kim, S. W. Kim, C. Y. Kang, S. J. Yoon, and Y. S. Kim, *Adv. Mater.* **24**, 6022 (2012).
- ⁴¹Y. Zhang, Y. Liu, and Z. L. Wang, *Adv. Mater.* **23**, 3004 (2011).
- ⁴²Y. Liu, Y. Zhang, Q. Yang, S. M. Niu, and Z. L. Wang, *Nano Energy* **14**, 257 (2015).
- ⁴³R. F. Pierret, *Semiconductor Device Fundamentals* (Addison-Wesley, Massachusetts, 1996).
- ⁴⁴H. F. Tiersten, *Linear Piezoelectric Plate Vibrations* (Springer Science, New York, 1969).
- ⁴⁵W. Z. Wu and Z. L. Wang, *Nat. Rev. Mater.* **1**, 16031 (2016).